Electromagnetic Modeling and Design of Dual-Band Septum Polarizers

Anatoliy A. Kirilenko[1], Dmitriy Yu. Kulik[1], Leonid A. Rud[1], Vladimir I. Tkachenko[1], and Naftali Herscovici[2]

[1]Institute of Radiophysics and Electronics
National Academy of Sciences of Ukraine
Kharkov, 61085, Ukraine

[2]Atlantic Microwave Co.
Bolton, MA 01740-1196, USA

***Abstract*—**A highly efficient, full-wave electromagnetic model and CAD of septum polarizers terminated with a square or circular output waveguide is presented. The model is based on the mode-matching and generalized S-matrix techniques. The capabilities of the CAD program are demonstrated by the design of dual-band polarizers where the separation between two bands is more than 50%. For a square output polarizer, results are compared and found to be in good agreement with data obtained with the WASP-NET program. A discussion on the inherent limitations of the achievable performance and critical parameters is presented. An influence of higher-order modes propagating in the polarizer output over the high-frequency operation band on the radiation and polarization patterns of a septum polarizer combined with a corrugated conical horn is specially investigated.

I. INTRODUCTION

Septum polarizers (SP), built on a square waveguide with stepped ridged waveguide junctions, have found many applications in antenna and other microwave systems. Single-band configurations with a square output waveguide were widely investigated. The four-step polarizer, initially designed in [1] by trial and error experimental methods, satisfied the return loss criteria but required an additional dielectric-slab phase shifter to adjust the 90-degree phase difference between the TE_{10} and TE_{01} orthogonal modes. There were difficulties in producing an acceptable phase shift with an experimental tuning of the polarizer without phase-adjusting structures, [2].

Full-wave solutions and numerical optimization procedures allowed the design of various single-band polarizers with a square output port that met the required characteristics over a broad bandwidth. The design results of a five-step septum polarizer without an additional phase adjustment were reported in [3]. A section of corrugated waveguide was proposed to use as the phase-correction device, [4]. The broadband polarizers with a stepped-thickness septum were investigated in [5], [6]. A dynamical optimization procedure that included in the optimization process not only the stepped septum configuration but also several step discontinuities (placed before and after the septum) was proposed in [7]. An algorithm based on the approximation of aperture field distribution by Gegenbauer polynomials was used in [8] to analyze the SP experimentally studied in [6].

The septum polarizer with a circular output port is more convenient for antenna applications because it can be connected directly to a flange of smooth or corrugated conical horn. An example of the design of a square septum polarizer, which is directly combined with a smooth conical circular waveguide horn, is shown in [9]. A design procedure for the single-band polarizer with a circular output waveguide is discussed in [8] however results of this design were not presented. Some results are reported in [10] for compact three- and four-step polarizers.

To the authors' knowledge, except for [11], dual-band septum polarizers operating over two distant (with more than 15% separation) frequency bands have not been yet considered in the literature. In addition to the need to meet common requirements (such as return loss, isolation, and axial ratio performance), in this case a new parameter has to be considered: the level of suppression of the higher-order modes. These modes are always excited and can propagate over the high-frequency band. In the case of square output port, these modes are the TE_{11} and TM_{11} ones, and in the case of circular output port they are the axial-symmetric TM_{01} and two polarization-degenerated TE_{21} modes.

In the present paper, the electromagnetic model, optimization procedure, designing results for the dual-band polarizers with square or circular output waveguides, and some features of their characteristics are discussed.

II. DESIGN PROCEDURE

II.1. The Electromagnetic Model

A polarizer with a circular output waveguide and its geometrical parameters are shown in Fig. 1. The electromagnetic model is based on the generalized *S*-matrix technique. In applying this technique, the key-elements are identified with the following waveguide discontinuities:

- double step in a rectangular waveguide;
- bifurcated–to–ridged waveguide transition;
- ridged-to-ridged waveguide junction;
- square-to-square waveguide junction;
- square-to-circular waveguide transition.

The full-wave *S*-matrices of all the key-elements are calculated using the mode-matching technique. In the case when the jointed circular and square waveguides have overlapping cross-sections (as shown in Fig. 1(a)), this transition is considered as two waveguides connected via a zero-length square waveguide with the wall size $a_{virt} = D$ where D is the diameter of the output circular waveguide. In this case, the circular output is circumscribed to the virtual square waveguide. All the aforementioned key-elements are calculated and combined with the aid of an electromagnetic solver similar to the one reported in [12]. The eigen-value problem for the single-ridged waveguide is solved using the moment method with basis and test functions that take into account the field behavior near edges. Some details of this method can be found in [13].

II.2. The Optimization Procedure

The SP-CAD program allows the design of a dual- and single-band polarizer according to a given set of specifications such as:

- return loss (*RL*);
- isolation (*IS*) between input waveguides;
- axial ratio (*AR*) of the resulting field generated by two outgoing orthogonal dominant modes;
- suppression level (*SL*) of the higher parasitic modes in the output port if the latter is overmoded.

The used optimization procedure is based on the descent method.

The SP-CAD program operates with the given number of polarizer components. Some of them are fixed, and others are changed during the optimization process. For a given number of septum steps *N*, the fixed geometrical parameters are:

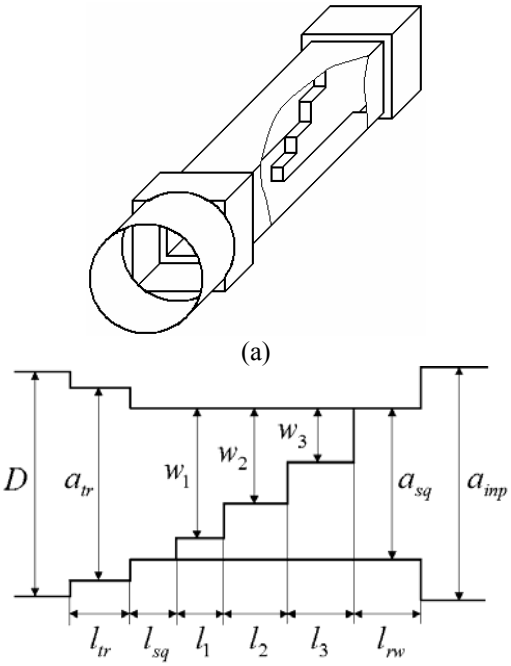

Fig. 1. Schematic structure of a three-step polarizer with a circular output waveguide. (a) General view, (b) Longitudinal-section view.

- the cross-sections of the two identical input rectangular waveguides, $a_{inp} \times b_{inp}$;
- the septum thickness, t;
- the size of a square housing for the ridged waveguide sections, $a_{sq} \times a_{sq}$;
- the size of the transformer square section, $a_{tr} \times a_{tr}$, placed between the above-mentioned housing and output circular waveguide;
- the diameter of the circular waveguide, D.

The other available SP configurations have the square output port with $a_{out} = a_{tr}$.

Generally, the gap sizes w_i and lengths l_i, $i = 1, 2, ..., N$ of the single-ridged waveguide sections, the length l_{rw} of the two identical rectangular waveguides of the $a_{inp} \times \left(a_{sq} - t\right)/2$ cross section, and the lengths l_{sq} and l_{tr} of the square waveguide sections (see Fig. 1(b)) are included in the vector of objective variables for the

optimization procedure. The following error function is minimized during the optimization:

$$F(\vec{x}) = \min \sum_{j=1}^{2} \sum_{m=1}^{M_j} \left[W_{RL}^{(j)} \left(\frac{RL_j}{RL_m^{(j)}} \right)^2 + W_{IS}^{(j)} \left(\frac{IS_j}{IS_m^{(j)}} \right)^2 + W_{AR}^{(j)} \left(\frac{AR_m^{(j)}}{AR_j} \right)^2 + W_{SL}^{(j)} \left(\frac{SL_j}{SL_m^{(j)}} \right)^2 \right] \quad (1)$$

where

- $\vec{x}$ is the vector of the objective variables;
- M_j is the given number of the frequency points $f_m^{(j)}$ within the *j*th specified band;
- $W_{RL}^{(j)}$ is the return loss weighting coefficient;
- RL_j is the specified return loss value (in dB);
- $RL_m^{(j)} = RL_m^{(j)}\left(f_m^{(j)}, \vec{x}\right)$ is the actual return loss value calculated at the frequency $f_m^{(j)}$ and with the current values of the objective variables.

The similar notations are used in (1) for the other controlled characteristics.

II.3. The Initial Guess

To the authors' knowledge, there are no well established models that can be applied for the preliminary SP synthesis. As in any multivariable optimization routine based on gradient or descent methods, the selection of the initial guess is the most difficult problem. Various approaches can be adopted to overcome this problem. The first of them consists in the electrical scaling of a known SP geometry (for example, from [1] to a new frequency operation band. This approach can be used for a simple configuration representing a stepped septum in a straight square waveguide (as in [1], [3]).

With the SP-CAD, the choice of the invariable polarizer dimensions is based on the following considerations. The square housing size a_{sq} must be such that the cutoff frequency of the TE_{11} and TM_{11} modes in the hollow $a_{sq} \times a_{sq}$ waveguide is between the polarizer operation bands. Preferable size a_{out} for the SP with a square output waveguide is that permits to propagate the higher TE_{11} and TM_{11} modes over the high-frequency band only.

If the SP with a circular output is required, the output diameter *D* can be chosen using similar considerations. In the last case, the recommended size of square transformer section a_{tr} is such that the cutoff frequencies of dominant modes in the circular and transformer waveguide section are close to each other. This takes place if $a_{tr} \approx 0.85D$.

A simple way to define the initial septum geometry is to define the ridge gap dimensions according to the linear representation (for example) such as $w_i = a_{sq}\left(1 - i/(N+1)\right)$, $i = 1, 2...N$. The lengths of the corresponding waveguide sections can be set as $l_i = (0.4 - 0.5)a_{sq}$.

II.4. The Surrogate Models

The SP-CAD allows two options: the optimization can be done either with the *exact numerical models* of all components or with *interpolated models* of the generalized *S*-matrices of some components (called here "*surrogate"* models).

Before starting the optimization process, one-dimensional *frequency buffers* are created for the exact *S*-matrices of the polarizer components with *fixed geometry*. For example, for a square-to-circular waveguide transition, the buffer is calculated at the given set of frequency points $f_m^{(j)}$ only once, and is not recalculated during the optimization process.

The exact models of polarizer components with *varying geometry* (such as the ridged-to-ridged waveguide junctions) are substituted by their *two-dimensional surrogates*. The latter are obtained by the interpolation of the full-wave *S*-matrices of the above-mentioned junctions at a given set of sampling points for geometrical parameters at each frequency $f_m^{(j)}$. In this case, the varied geometrical parameters are the sizes of gaps w_n, $n = 1, 2, ..., N$ of adjacent ridged waveguide sections. The calculation of the database for the surrogate models is a time-consuming procedure, but once the database is created, the overall CPU time used for the polarizer optimization is considerably reduced. The database is stored in files and can be used repeatedly to optimize polarizers differing only by the parameters a_{tr} and/or D.

The program can operate in various accuracy modes. The low-accuracy mode with using the surrogate models allows a rough evaluation of a certain SP topology. This mode is a fast and suitable way for the definition of the initial guess for the final optimization performed in the high-accuracy mode. The frequency

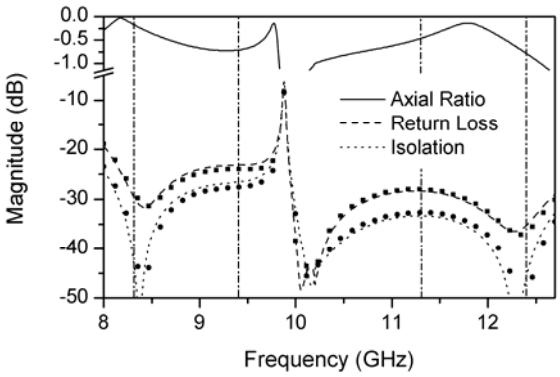

(a)

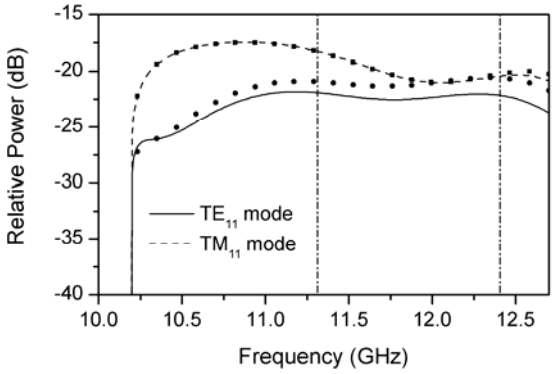

(b)

Fig. 2. Performance of the designed four-step WR-90 septum polarizer with a square output waveguide and comparison with the WASP-NET analysis. Dimensions (in millimeters): a_{inp} = 22.86, b_{inp} = 10.16, a_{sq} = 20.8, l_{rw} = 5.39, t = 1.5, w_1 = 17.23, l_1 = 9.03, w_2 = 13.85, l_2 = 9.53, w_3 = 10.48, l_3 = 8.46, w_4 = 4.83, l_4 = 3.72, a_{out} = 20.8.

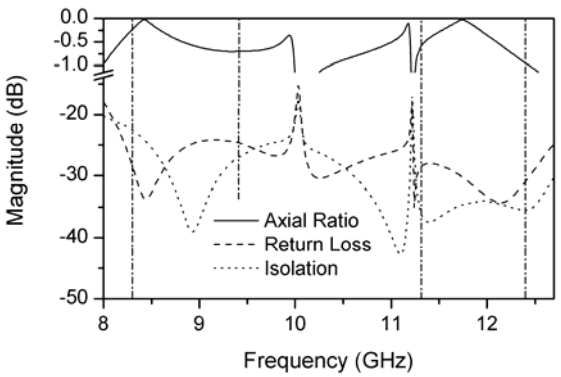

(a)

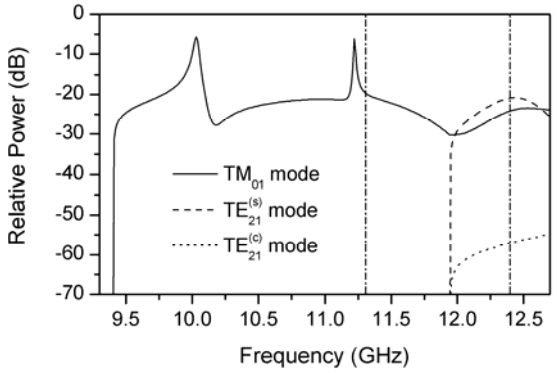

(b)

Fig. 3. Performance of the designed four-step WR-90 septum polarizer with a circular output waveguide. Dimensions (in millimeters): a_{inp} = 22.86, b_{inp} = 10.16, a_{sq} = 20.5, l_{rw} = 4.1, t = 1.5, w_1 = 17.11, l_1 = 9.77, w_2 = 14.03, l_2 = 10.16, w_3 = 10.68, l_3 = 8.35, w_4 = 4.57, l_4 = 3.45, l_{sq} = 5.8, a_{tr} = 21.6, l_{tr} = 8.48, D = 24.4.

analysis of the optimized SP is performed with using the exact numerical models of all the SP components in the chosen accuracy mode.

III. SOME RESULTS OF THE SP DESIGN

The SP-CAD program has been successfully applied in the design of polarizers having a square or circular output waveguide. The results for four-step optimized polarizers operating in several frequency ranges are presented in Figs. 2 to 5. They have been analyzed with the high-accuracy exact model under the SP dimensions shown in the figures captions. The SP operation bands are delimited in the figures by the vertical dashed-dotted lines. Figures marked as "(b)" show the axial ratio (*AX*), return loss (*RL*), and isolation (*IS*) polarizers performance whereas the "(b)" figures characterize the relative powers (suppression levels (*SL*)) of unwanted higher-order modes in the SP output.

The optimization of all the SPs has been carried out with the following specification within two bands:

- return loss $RL \le -20$ dB;
- isolation between the input waveguides $IS \le -25$ dB;
- axial ratio (calculated from the dominant modes amplitudes in the SP output) $AR \ge -1$ dB;
- higher-order mode suppression level $SL \le -20$ dB.

Figs. 2(a)-(b) show the predicted performances of the optimized square-output polarizer designed for two bands, 8.3 GHz - 9.4 GHz and 11.3 GHz - 12.4 GHz. Input ports are the WR-90 waveguides. The resulting characteristics are close to the specified ones within both bands. For comparison purposes, the numerical data obtained with WASP-NET program, described in

[14], and [15], are plotted by symbols in Figs. 2(a)-(b) as well. Good agreement between data obtained with two programs is evident. This is mainly due to the fact that both programs are based on the mode-matching technique and the calculations were carried out with the same frequency, $f_{\max} = 72$ GHz, limiting maximal cutoff frequencies of modes in ports of all the key-elements. Some differences at high frequencies are due to the following reasons. First, two programs uses the different algorithms in the calculation of the ridged waveguide modal basis. In addition, the number of modes taken into account between any connected discontinuities was set as twenty in the SP-CAD program when using the *S*-matrix technique. In the WASP program, this number is determined indirectly: all modes in connecting waveguide sections with cutoffs $f_{con} \le f_{\max}$ are taken into account. The WASP results in Fig. 2 were calculated at $f_{con} = 0.55 f_{\max}$.

A characteristic feature of the frequency responses shown in Fig. 2(a) is a sharp resonance at f = 9.88 GHz. It shows up before the cutoff frequency of the TE_{11} and TM_{11} modes ($f_{cut} \approx 10.19$ GHz) in the output waveguide (see Fig. 2(b)). When passing this frequency point, the TE_{10} mode transmission coefficient and axial ratio response decrease drastically and the differential phase shift exhibits a sharp jump. It is the resonance effect that limits the widths of the polarizer operation bands. This effect is due to the resonance of the first higher quasi-TE_{11} mode that propagates in the ridged waveguide sections and does not propagate in the input and output waveguides. Similar resonances are named as *resonances on higher "ghost"* (or *"closed"*) *modes* and have been studied in the literature (see, for example, [16], [17]). The discussed resonance has been experimentally observed in [3] and specially noted in [5] when analyzing single-band SPs. It is an inherent feature of the SPs and cannot be avoided. One can only control the resonance frequency value by a proper choice of the SP size a_{sq}.

The results for the optimized WR-90 SP with a circular output waveguide are shown in Fig. 3. The return loss, isolation, and axial ratio responses meet the specification over the two specified bands practically (see Fig. 3 (a)). The circular output diameter for this SP is chosen so that the parasitic TM_{01} mode cutoff ($f_{cut} = 9.41$ GHz) is outside the low-frequency band and the TE_{21} cutoff ($f_{cut} = 11.94$ GHz) is within the high-frequency band. The curves of the parasitic mode powers are shown in Fig. 3(b). There are two TE_{21} modes, $TE_{21}^{(s)}$ and $TE_{21}^{(c)}$, which transversal field components are orthogonal and rotated by 45° relative to each other. Here, the superscript *s* or *c* denotes the $\sin n\varphi$ or $\cos n\varphi$ polar-angle function, respectively, in the Herz vector representation for the modes in a circular waveguide. It is remarkable that the level of the $TE_{21}^{(s)}$ mode is considerably higher than the $TE_{21}^{(c)}$ one. This is caused by that the $TE_{21}^{(s)}$ mode is efficiently excited by the TE_{11} mode propagating in the SP square waveguide sections because both these modes have similar field distributions.

In contrast to the polarizer with a square output, the frequency responses in Fig. 3 (a) have two resonances. The first of them has the same nature as that in Fig. 2 (a). The second resonance appears before the beginning of high-frequency band. It is caused by the transformer square section TE_{11} mode coupled with the $TE_{21}^{(s)}$ mode in the circular output waveguide and playing a role of that closed in the SP cavity. This resonance is a reason of an increased level of the TM_{01} mode before the high-frequency band (see Fig. 3 (b)). To shift the resonance to a lower frequency, a larger output diameter has to be chosen. However, in this case the TM_{01} mode starts to propagate within the low-frequency band that is not acceptable for some SP applications. A similar resonance peak does not appear before the TM_{01} mode cutoff. This mode is excited by the TM_{11} mode of the transformer square section with the cutoff frequency higher than the TM_{01} one. In this case, there are no closed modes and a resonance has not to be appeared, [17]. The aforementioned resonances can lead to some difficulties in designing the SP with a circular output port at a smaller separation between two bands.

The separation between the bands of the aforementioned polarizers is 46% with respect to the total SP operation range and both these bands are within the WR-90 waveguide frequency range. Figs. 4 and 5 demonstrate the SP-CAD capabilities in designing the millimeter-wave polarizers provided with the input WR-34 rectangular waveguides and operating over the bands 20 GHz - 21.5 GHz and 29.5 GHz - 31.5 GHz. The SPs have been designed under the performance specification identical to that for the WR-90 polarizers. The separation between the bands already is about 70%. It should be noted that the low-frequency SP band is entirely outside of the standard frequency range (22 GHz-33 GHz) of the WR-34 waveguide.

The square-output SP performance shown in Figs. 4

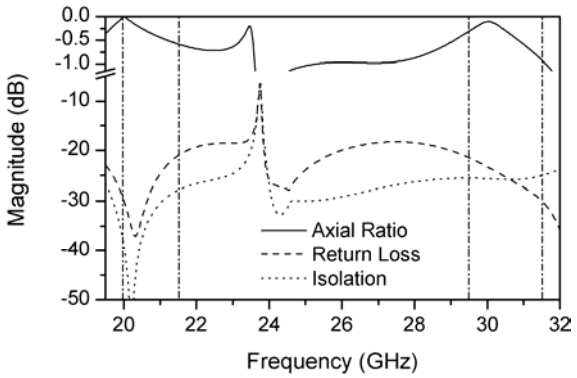

(a)

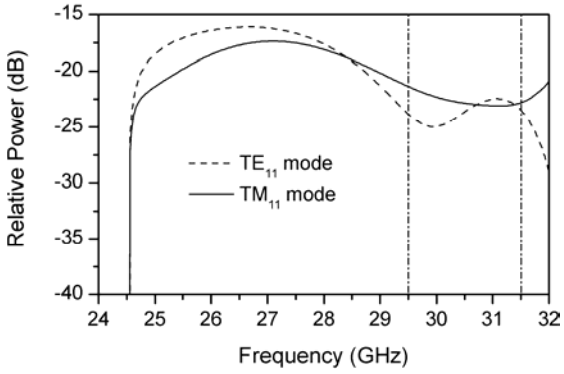

(b)

Fig. 4. Performance of the designed four-step WR-34 septum polarizer with a square output waveguide. Dimensions (in millimeters): a_{inp} = 8.636, b_{inp} = 4.318, a_{sq} = 8.636, l_{rw} = 8.70, t = 1.0, w_1 = 7.10, l_1 = 3.45, w_2 = 5.90, l_2 = 3.84, w_3 = 4.61, l_3 = 3.73, w_4 = 2.58, l_4 = 1.63, a_{out} = 8.636.

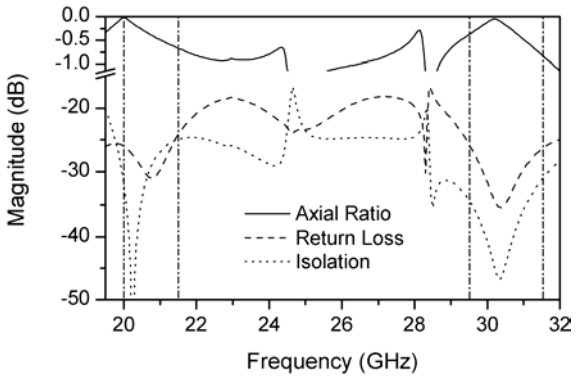

(a)

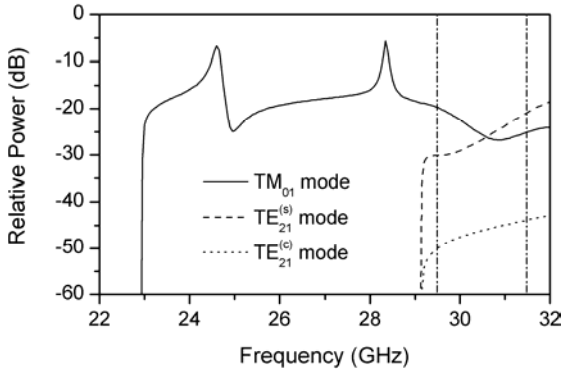

(b)

Fig. 5. Performance of the designed four-step WR-34 septum polarizer with a circular output waveguide. Dimensions (in millimeters): a_{inp} = 8.636, b_{inp} = 4.318, a_{sq} = 8.40, l_{rw} = 9.27, t = 1.0, w_1 = 6.88, l_1 = 3.52, w_2 = 5.63, l_2 = 3.65, w_3 = 4.34, l_3 = 3.40, w_4 = 1.95, l_4 = 1.43, l_{sq} = 1.07, a_{tr} = 8.6, l_{tr} = 2.57, D = 10.0.

(a)-(b) meet the specifications over two bands. The designed circular-output SP has the characteristics close to the specified ones as well (see Fig. 5). This follows partly from a fact that the bands are widely separated and the second resonance is sufficiently far from the beginning of high-frequency band in contrast to the SP of Fig. 3.

IV. THE ANALYSIS OF POLARIZER WITH CORRUGATED HORN

Though the above-discussed higher-order modes are low in power, the following question has to be studied specially: how do they influence the resulting axial ratio value in the SP output? As an example, let us consider the SP illustrated by Fig. 3. For this SP, one (TM_{01}) or three (TM_{01}, $TE_{21}^{(c)}$, and $TE_{21}^{(s)}$) higher-order modes can propagate in the circular output over the 11.3 GHz – 11.94 GHz or 11.94 GHz – 12.4 GHz subbands of the high-frequency band, respectively (see Fig. 3 (b)).

We will further emphasize the second subband because of the greater number of higher-order propagating modes there. One can see that within this subband the TM_{01} and $TE_{21}^{(s)}$ modes are excited with comparable amplitudes that are essentially higher than the $TE_{21}^{(c)}$ mode one. However, these modes have the field component distributions and propagation constants differing from each other and from those of the dominant $TE_{11}^{(s)}$ and $TE_{11}^{(c)}$ modes. This will leads to a different axial ratio of the polarization ellipse of the

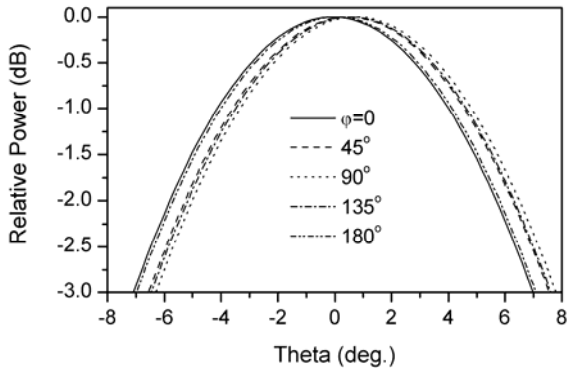

(a)

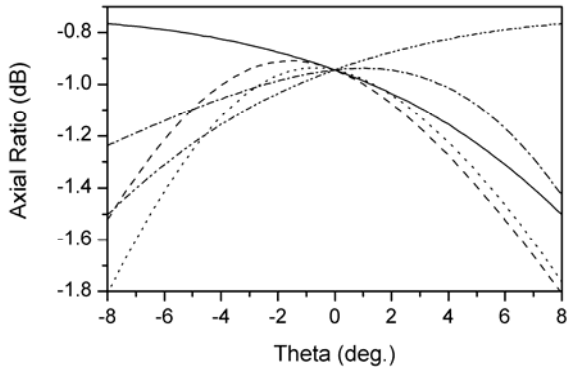

(b)

Fig. 6. The radiation (a) and polarization (b) patterns of the cascade consisting of the septum polarizer and corrugated conical horn.

entire field, i.e. including all the propagating higher-order modes, calculated at an arbitrary point of the SP circular output cross-section and at different distances from the output beginning. The axial ratio at any point of the output waveguide axis has to be equal to that calculated from the dominant modes amplitudes because the electrical field components of the considered higher-order modes are zero at the axis.

Due to the aforementioned entire field properties, it is difficult to obtain a certain answer to the above-put question. Such a conclusion is valid for the first subband with one high-order TM_{01} mode as well. More objective information can be obtained from the analysis of far field radiation and polarization patterns for a cascade of the septum polarizer and corrugated horn. A dual-band corrugated conical horn has been previously designed for two frequency bands identical to those for the polarizer of Fig. 3 using a numerical procedure reported in [18]. The horn is characterized by the following parameters: input waveguide diameter $D_{inp} = 24.4$ mm, aperture diameter $D_{horn} = 132$ mm, semi-flare angle $\alpha = 15°$, throat circular waveguide section of the diameter D_{inp} and the length l. Eight modes are taken into account in this section. It should be noted that the value of l influences essentially the radiated field characteristics.

The radiation and polarization patterns of the polarizer-horn cascade with $l = 8.7$ mm are shown in Fig. 6(a) and 6(b), respectively. They are computed at $f = 12.4$ GHz for several φ-planes within the 3-dB θ-angle sector. At the considered frequency, the polarizer has the worst axial ratio value $AX = -0.94$ dB calculated from the dominant modes amplitudes and comparable amplitudes of the propagating TM_{01} and $TE_{21}^{(s)}$ higher-order modes (see Fig. 3). Just these modes result in a deviation of the radiation pattern maximum (up to $\Delta\theta = 0.8°$ at $\varphi = 90°$) from the axial direction $\theta = 0$ (Fig. 6(a)) and in an asymmetry of the polarization patterns in different φ-planes (Fig. 6 (b)). As expected, the axial ratio curves intersect at the point $\theta = 0$ for all the φ-planes on the level equal to that for the polarizer (compare Fig. 3 (b) at f = 12.4 GHz and Fig. 6 (b) at $\theta = 0$). This is because the fields of higher-order modes do not make a contribution to the polarization patterns in the axial direction $\theta = 0$. The symmetry condition of type $F(\varphi, \pm\theta) = F(180° + \varphi, \mp\theta)$ is carried out for the relative power and axial ratio dependences on θ (for example, see curves for $\varphi = 0$ and $\varphi = 180°$ in Fig. 6(a) and 6(b)).

One would expect that the similar features are valid for the radiation and polarization patterns of SPs with a square output as well.

V. CONCLUSION

The results presented in this paper show the capabilities of the SP-CAD program as a tool for efficient and accurate design of compact waveguide septum polarizers terminated with square or circular output waveguides and operating in two distant frequency bands. The SP-CAD produces results that are in good agreement with those calculated with an extensively validated electromagnetic solver. The nature of the resonance effects limiting the bandwidths of different polarizer configurations is discussed. The influence of propagating higher-order modes on characteristics of the far field radiated from a corrugated conical horn terminating a polarizer is analyzed. It is found that

higher-order modes produce a deviation of the radiation pattern maximum and an asymmetry of the polarization pattern relative to the axial direction.

ACKNOWLEDGMENT

The authors would like to thank Prof. F. Arndt, University of Bremen, Germany, for his kind contribution in analyzing the septum polarizers with WASP.

REFERENCES

[1] Chen M.H. and G.N. Tsandoulas, "A wide-band square-waveguide array polarizer," *IEEE Trans. Antennas Propag.*, vol. 21, pp.389-391, May 1973.

[2] Ege T. and P. McAndrew, "Analysis of stepped septum polarizers," *Electron. Lett.*, vol. 21, pp. 1166-1168, Nov. 1985.

[3] Esteban J. and J.M. Rebollar, "Field theory CAD of septum OMT-polarizer," in *1992 IEEE AP-S Int. Symp. Dig.*, pp. 2146-2149.

[4] Ihmels R., U. Papziner, and F. Arndt, "Field theory design of a corrugated septum OMT," in *1993 IEEE MTT-S Int. Microwave Symp. Dig.*, pp. 909-912.

[5] Bornemann J. and V. Labay, "Ridged waveguide polarizers with finite and stepped-thickness septum," *IEEE Trans. Microwave Theory Techn.*, vol. 43, pp.1782-1787, Aug. 1995.

[6] Bornemann J. and S. Amari, "Septum polarizer design for antenna feeds produced by casting," in *1997 IEEE AP-S Int. Symp. Dig.*, pp. 1422-1425.

[7] Piovano B., G. Bertin, L. Accatino, and M. Mongiardo, "CAD and optimization of compact wide-band septum polarizers," in *Proc. 29th Europ. Microwave Conf.*, vol. 3, Munich, Germany, Oct. 1999, pp. 235-238.

[8] Bouki-Hacene N., J. Sombrin, and A. Papiernik, "Approximation by Gegenbaur polynomials in the study of a rectangular ridged waveguide. Application to the analysis of a waveguide septum polarizer," *Int. J. Numerical Modeling*, vol. 16, pp. 299-318, Apr. 2003.

[9] Beyer R. and F. Arndt, "Efficient hybrid mode-matching/-finite-element (MM/FE) method for the design of waveguide components and slot radiators," in *1998 IEEE MTT-S Int. Microwave Symp. Dig.*, pp. 1275-1278.

[10] Kirilenko A.A., D.Yu. Kulik, L.A. Rud, V.I. Tkachenko, and N. Herscovici, "Compact septum polarizers with a circular output waveguide," in *Proc. 5th Int. Kharkov Symp. Physics and Engineering of Microwave, MM, and SubMM Waves, MSMW'04*, Kharkov, Ukraine, June 2004, pp. 686-688.

[11] Kirilenko A., D. Kulik., L. Rud, V. Tkachenko, and N. Herscovici, "CAD of double-band septum polarizers," in *Proc. 34th Eur. Microwave Conf.*, Amsterdam, Netherlands, Oct. 2004, pp. 277-280.

[12] Kirilenko A., D. Kulik, Yu. Parkhomenko, L. Rud., and V. Tkachenko, "Automatic electromagnetic solvers based on mode-matching, transverse resonance, and S-matrix technique," in *Proc. XIV Int. Conf. Microwaves, Radar and Wireless Communications, MICON-2002*, Gdansk, Poland, May 2002, pp. 815-824.

[13] Kirilenko A.A., L.A. Rud, and V.I. Tkachenko, "CAD of evanescent-mode band-pass filters based on the short ridged waveguide sections," *Int. J. RF Microwave CAE*, vol. 8, pp.354-365, Nov. 2001.

[14] MIG, Microwave Innovation Group, "A CAD tool utilizing fast hybrid MM/FE/MoM/FD techniques," *Microwave Journal*, vol. 45, 178-180, Sept. 2002.

[15] Arndt F., J. Brandt, V. Catina, J. Ritter, I. Rullhusen, J. Dauelsberg, U. Hilgefort, and W. Wessel, "Fast CAD and optimization of waveguide components and aperture antennas by hybrid MM/FE/MoM/FD methods – state-of-art and recent advances," *IEEE Trans. Microwave Theory Techn.*, vol. 52, pp. 292-302, Jan. 2004.

[16] Jaynes E.T., "Ghost modes in imperfect waveguides," *Proc. IRE*, vol. 46, pp. 416-418, Feb. 1958.

[17] Shestopalov V.P., A.A. Kirilenko, and L.A. Rud', *Resonance Wave Scattering. Vol. 2. Waveguide Discontinuities.* Kiev: Naukova Dumka, 1986, ch. 4, 5.

[18] Perov A., L. Rud, S. Senkevich, and V. Tkachenko, "Automated design of corrugated conical horns for dual-band applications," in *Proc. 10th Int. Conf. Mathematical Methods in Electromagnetic Theory, MMET-04*, Dniepropetrovsk, Ukraine, Sept. 2004, pp. 478-480.

Anatoliy A. Kirilenko was born in Tambov, Russia, in 1943. He was graduated from the Radiophysics Department of the Kharkov State University, Ukraine, in 1965. He received the Ph.D. and D.Sc. degrees from the Kharkov State University, in 1970 and 1980, respectively, and Professor title in radiophysics from the Academy of Sciences, USSR, in 1989.
Since 1965, he has been with the Institute of Radiophysics and Electronics, National Academy of Sciences of Ukraine, Kharkov, where he is currently a Head of the Department of Computational Electromagnetics. Since 1981, he is a Professor of the National Aerospace University, Kharkov. His research interests are analytical and numerical methods in electromagnetics, resonance phenomena in waveguides and gratings, microwave CAE and CAD.
Prof. Kirilenko is a Winner of the 1989 State Prize of Ukraine in the field of Science and Technology and a recipient of the 1991 award for the best software in the field of microwave electronics in the former USSR.

Dmitriy Yu. Kulik was born in Kharkov, Ukraine, in 1965. He received the Radioelectronics Engineering degree from the Kharkov Aviation Institute, in 1988 and Ph.D. degree in radiophysics from the Institute of Radiophysics and Electronics, National Academy of Sciences of Ukraine, Kharkov, in 2003.
From 1988 to 1993, he was with the Radar Department, from 1993 to 1998, with the Center of Remote Sensing of Earth, and since 1998, with the Department of Computational Electromagnetics of the Institute of Radiophysics and Electronics, where he is currently a Researcher Scientist. His research interests are a computer simulation of microwave devices, development of the software for designing waveguide filters and diplexers.

Leonid A. Rud was born in the Donetsk region, Ukraine, in 1946. He received the Radiophysics Engineering degree from the Kharkov Institute of Radioelectronics, in 1964, Ph.D. and D.Sc. degrees in radio-physics from the Kharkov State University, in 1976 and 1990, respectively, and the Senior Scientist title in radiophysics from the Academy of Sciences, USSR, in 1984.
Since 1971, he has been with the Institute of Radiophysics and Electronics, National Academy of Sciences of Ukraine, Kharkov, where he is currently a Leading Scientist of the Department of Computational Electromagnetics. His research interests include the mathematical simulation of wave scattering from waveguide discontinuities, spectral theory of open waveguide resonators, CAD of waveguide and antenna components, frequency-selective devices.
Dr. Rud is a Winner of the 1989 State Prize of Ukraine in the field of Science and Technology.

Vladimir I. Tkachenko was born in Lviv, Ukraine, in 1951. He received the Researcher and Ph.D. degrees in radio-physics from the Kharkov State University, in 1973 and 1986, respectively.
From 1973 to 1981, he was with the Low Temperature Physics Institute, National Academy of Sciences of Ukraine, Kharkov, where he was involved in the development of superconductive antennas theory. In 1981, he joined the Institute of Radiophysics and Electronics, the National Academy of Sciences of Ukraine, Kharkov, where he is currently a Senior Scientist of the Department of Computational Electro-magnetics. From 1991 to 1996, he was an Assistant Professor at the Kharkov State Technical University of Radioelectronics. His research interests are numerical algorithms and software for the design of microwave devices and large-scale modeling software for the waveguide systems.
Dr. Tkachenko is a recipient of the 1991 award for the best software in the field of microwave electronics in the former USSR.

Naftali Herscovici was born in Bucuresti, Romania, in 1954. He received his B.Sc., M.Sc. from the Technion, Haifa, Israel and his Ph.D. from the University of Massachusetts, Amherst, in 1978, 1985 and 1992, respectively.
Between 1982 and 1989 he was employed by Rafael, Haifa, Israel as an Antenna Research Engineer; there he was engaged in research and development of microwave antennas. He is currently the Director of the Antenna Department at Atlantic Microwave, Bolton, MA USA. He is the author of over 50 technical papers in various journal and conference publications. His research interests include microstrip antennas and arrays, reflector antennas and feeds, pattern synthesis and antenna modeling.